Advances in Adaptive Data Analysis
Vol. 3, No. 3 (2011) 325–338

DOI: 10.1142/S1793536911000702

World Scientific
www.worldscientific.com

A NOVEL SIGNAL DECOMPOSITION APPROACH — ADAPTIVE FOURIER DECOMPOSITION

LIMING ZHANG

Faculty of Science and Technology,
University of Macau,
Av. Padre Tomas Pereira, Taipa, Macao, China
lmzhang@umac.mo

HONG LI

School of Mathematics and Statistics,
Huazhong University of Science and Technology,
Wuhan, Hubei province, China
hongli@hust.edu.cn

This paper presents a novel signal decomposition approach — adaptive Fourier decomposition (AFD), which decomposes a given signal based on its physical characters. The algorithm is described in detail, that is based on recent theoretical studies on analytic instantaneous frequencies and stands as a realizable variation of the greedy algorithm. The principle of the algorithm gives rise to fast convergence in terms of energy. Effectiveness of the algorithm is evaluated by comparison experiments with the classical Fourier decomposition (FD) algorithm. The results are promising.

Keywords: Signal processing; Fourier transform; signal decomposition.

1. Introduction

Signal processing is a fundamental tool in many engineering and scientific analyses. The applications span a large number of disciplines that include entertainment, communications, space exploration, medicine, archeology, geophysics, and so on [Oppenheim and Schafer, 2010]. The purpose of signal processing is to extract information from the original signal to reveal the underlying mechanism of various physical phenomena. The efficiency and quality of the signal processing depend strongly on the signal decomposition approach. The Fourier transform is a classic signal decomposition model, which has been applied to many different kinds of applications. It is well accepted because it has mathematical roots in analytic functional property, representing complicated signals into the physically realizable basic signals of meaningful instantaneous frequencies. By physically realizable, it means that they are boundary values of analytic functions, while by meaningful

instantaneous frequency, it amounts to say that in their polar coordinate representations, their phase derivatives are nonnegative (positivity of analytic phase derivative, referred as "mono-component" below).

Although Fourier transformation is widely used, some restrictions have been well noted. For a given signal, the Fourier inverse transformation expresses it into a linear combination of simple but fixed sine and cosine functions. Such expansions are argued that they cannot accurately represent local characteristic properties, especially the time-varying frequencies, of the given signal. Another restriction is that the decomposition may lead to slow convergence due to the fact that the principal sine and cosine components contributing significant shares of the total energy of the original signal may arrive late.

We treat four types of Hardy H_2 spaces of analytic functions, including one inside the unit circle (inner disc Hardy H_2 space), and one outside the unit circle (outer disc Hardy H_2 space), one above the real line (upper plane Hardy space), and one below the real line (lower plane Hardy space). They play important roles in our theory and algorithm. For knowledge on Hardy spaces in general we refer to [Garnett, 1987; Rudin, 1996]. In the circle case, for instance, the inner Hardy space consists of the analytic functions inside the unit circle possessing square-integrable nontangential maximal functions on the circle. There exists an isometric isomorphism between those analytic functions in the Hardy space and their boundary values. The inner and outer Hardy spaces are orthogonal to each other. The inner Hardy space, in particular, is the set of the square-integrable functions whose Fourier series are of the form $s(t) = c_0 + c_1 e^{it} + \cdots + c_n e^{int} + \cdots$. That is, the terms corresponding to negative powers of e^{it} are absent in the series expansion. We use the notation H_2 for each of the above-mentioned Hardy spaces. In the present paper, we concentrate in the inner disc H_2 space. It is proved that any square-integrable function s on the circle can be decomposed into a sum of two functions $s = s^+ + s^-$, in which s^+ is the boundary value of a function in the inner disc Hardy space and the other, s^-, is the boundary value of one in the outer disc Hardy space. The present paper devotes the adaptive Fourier decomposition (AFD) algorithm for s^+ and s. The relation between a real-valued function s and its Hardy space projection s^+ is

$$s = 2\mathrm{Re}\{s^+\} - c_0, \tag{1}$$

where c_0 is the average of the function on the unit circle [Qian and Wang, 2010]. Due to this relation, the decomposition of a real-valued signal s is reduced to that of its Hardy space projection. For functions on the line, there is a parallel theory that uses upper- and lower-plane Hardy spaces. Signals belonging to the Hardy spaces are called analytic signals. For a given signal s, its associated *analytic signal* is $2s^+$. For knowledge on Hardy spaces and analytic signals in general, we refer to the paper by [Garnett, 1987].

The next important concept in the AFD approach is *mono-component*, defined as follows [Qian, 2006; 2010]. A function (or signal), $s(t)$, no matter being

complex- or real-valued, is said to be a mono-component, if $s(t) + iHs(t)$, as the boundary value of a function in H_2, where H is the Hilbert transform of s, with the amplitude-phase representation $s(t)+iHs(t) = \rho(t)\exp(i\theta(t))$ there holds $\theta^{'}(t) \geq 0$. The *analytic phase derivative* $\theta^{'}(t)$ is called the *instantaneous frequency* if and only if the requirement $\theta^{'}(t) \geq 0$ is met, or, equivalently, s is a mono-component.

The Hilbert transformation involved in the definition is a crucial subject [Garnett, 1987; Rudin, 1996]: a function $s = u + iv$, where u, v are real-valued, with certain integrability condition, is the boundary value of an analytic function in the corresponding Hardy space if and only if $v = Hu$ [Qian, 2006].

A complex-valued signal is called a *pre-mono-component* [Qian, 2006; 2010] if there exists a positive number M such that $e^{iMt}s(t)$ is a mono-component. In the signal processing language, it means that riding on a carrier frequency e^{iMt}, or after a phase modulation by e^{iMt}, $M > 0$, the signal becomes a mono-component. Obviously, every mono-component is a pre-mono-component.

The novel signal decomposition approach — AFD is proposed in Qian [2010] and Qian and Wang [2010] with proven mathematical foundations. The present paper stresses on algorithm. The AFD approach is designed to treat the above-mentioned two restrictions of the Fourier transformation. In the algorithm, the building mono-components are adaptively selected based on the given signal under maximal projection principle. Such decompositions, therefore, can represent certain characteristic properties of the given signal. Applications of the AFD algorithm have appeared, for instance in H^{∞}-control theory [Mi and Qian, 2010]. Some experimental results are illustrated in the paper. The results show that the decomposition is of remarkable advantage.

This paper is organized as follows. The mathematical foundation and the AFD algorithm principle are introduced in Sec. 2. The algorithm is presented in detail in Sec. 3. The experimental results are shown in Sec. 4. The conclusions are drawn in Sec. 5.

2. Mathematical Foundation of the AFD

Let $G(z)$ be a function in H_2, or, equivalently, an analytic signal of finite energy. Assume that B_n are of the form

$$B_n(z) = \frac{\sqrt{1-\mid a_n \mid^2}}{1-\overline{a}_n z} \prod_{p=1}^{n-1} \frac{z-a_p}{1-\bar{a}_p z}, \quad n = 1, 2, \ldots, \tag{2}$$

where a_n are complex numbers inside the unit circle, $a_n = x + iy$, which are the parameters to be adaptively chosen in the algorithm. The system $\{B_n\}$ is called a Takenaka–Malmquist system or a rational orthogonal system [Akcay and Niness, 1999; Bultheel and Carrette, 2003; Bultheel *et al.*, 1999; Butzer and Nessel, 1971].

Note that in the expression

$$B_n(z) = O_n I_n, \tag{3}$$

where $O_n(z) = \sqrt{1-\mid a_n \mid^2}/1-\overline{a}_n z, I_n = \prod_{p=1}^{n-1} \frac{z-a_p}{1-\bar{a}_p z}$, the part I_n as a Blaschke product, is always a mono-component [Qian, 2010]. However, the part O_n is usually a pre-mono-component [Qian, 2010; Qian and Wang, 2010]. Therefore, their product, i.e. B_n, is always a pre-mono-component, and sometimes a mono-component.

It can be easily verified that if $a_{n_0} = 0$, then all B_n, $n \geq n_0$, are mono-components [Qian, 2010; Qian and Wang, 2010]. For historical notes on the system, we refer to the references cited in [Qian and Wang, 2010]. The maximal projection (matching pursuit) principle is as follows. Denote $e_{\{a\}} = B_1(z) = \sqrt{1-\mid a \mid^2}/1-\overline{a}z$. Then, for any $G \in H_2$, there exists an a_1 in the open unit disc $\mathbf{D}$ such that

$$|\langle G(z), e_{\{a_1\}}\rangle| = \max\{|\langle G, e_{\{a\}}\rangle| : a \in \mathbf{D}\}. \tag{4}$$

The AFD decomposition stands for the expansion

$$G(z) = \sum_{p=1}^{\infty} c_p B_p(z), \tag{5}$$

where c_p are the coefficients

$$c_p = \langle G, B_p\rangle = \int_0^{2\pi} G(e^{it})\overline{B_p(e^{it})}dt \tag{6}$$

where the parameters $a_1, \ldots, a_p$ are consecutively determined, by means of the optimization based on the maximal projection principle.

If compulsory selecting all $a_n = 0$, then Eq. (5) becomes the Fourier series decomposition. Thus, AFD is an optimization of the Fourier decomposition. The essence of the algorithm is to select the parameters according to the given signal to be decomposed. The maximal projection principle is in spirit of the so-called, and recently developed, matching pursuit or greedy algorithm [Mallat and Zhang, 1993]. The Hilbert space H_2 is with a linearly dense subset, called *dictionary*, consisting of the so-called evaluators, $e_{\{a\}}, a \in \mathbf{D}$.

They are of unit norms. The algorithm consecutively selects the evaluators, so that on their linear spans the given signal and the reduced remainders, respectively, attain the largest projections. The essence of the matching pursuit algorithm is the best selection "at each time." The maximal projection principle and convergence under the principle are two fundamentals of AFD [Qian, 2010; Qian and Wang, 2010].

In practice, the analytic signal to be decomposed is given by a set of discrete data on the boundary. Denote

$$G(e^{it_k}) = x_k, \quad k = 1, 2, \ldots, M, \tag{7}$$

where

$$t_k = 2\pi\Delta k, \quad \Delta = \frac{1}{M}, \quad t_k \in [0, 2\pi]. \tag{8}$$

First, we need calculate the energy of the given signal in terms of the data. Denote the energy of signal G by $\|G\|^2$, that is given by the norm of G in the Hilbert space.

The discretization of the integral formula for $\|G\|^2$ is

$$\|G\|^2 \approx 2\pi\Delta \sum_{k=1}^{M} |x_k|^2. \tag{9}$$

Through discretization of the integral formula (6), we have

$$|c_1|^2 = \left| \Delta \sqrt{2\pi(1-|a_1|)^2} \sum_{k=1}^{M} x_k \frac{1}{1-a_1 e^{-i2\pi\Delta k}} \right|^2. \tag{10}$$

According to the maximal projection principle, an a_1 exists that gives rise to the maximal value of $|c_1|^2$. To find a_1 maximizing $|c_1|^2$ is to solve a global extreme problem of a differentiable function in the unit disc. This can be done by the standard method in calculus. It can be done by MATLAB. Denote such $|c_1|^2$ by $\max|c_1|^2$, which is the energy of the first decomposition component G_1, where

$$G_1 = c_1 B_1 \tag{11}$$

$$B_1 = \frac{\sqrt{1-|a_1|^2}}{\sqrt{2\pi}} \frac{1}{1-\bar{a}_1 e^{it}}, \tag{12}$$

and $c_1 = \langle G, B_1 \rangle$.

Comparing the energy between the given signal and the output signal, $\|G\|^2 - \max|c_1|^2$, we can judge how close it is from the first partial sum to the original given signal. Then, repeat this process.

We have the following general relations.

$$|c_p|^2 = \left| \Delta \sqrt{2\pi(1-|a_p|^2)} \sum_{k=1}^{M} \frac{x_k}{1-a_p e^{-i2\pi\Delta k}} \prod_{q=1}^{p-1} \frac{1-\bar{a}_q e^{i2\pi\Delta k}}{e^{i2\pi\Delta k} - a_q} \right| \tag{13}$$

$$G_n = \sum_{p=1}^{n} c_p B_p, \tag{14}$$

where

$$c_p = \langle G, B_p \rangle. \tag{15}$$

The energy difference is calculated by the equation

$$\|G\|^2 - \sum_{p=1}^{n} \max|c_p|^2. \tag{16}$$

ADF for nonanalytic, and in particular, real-valued signals, is based on the relation (1). The algorithm is subject to further improvement. Now, the data (7) is given for the nonanalytic signal s, but the algorithm is for the analytic signal $G = s^+$. We first deduce [Qian, 2010].

$$\|G\|^2 \approx \pi\Delta \sum_{k=1}^{M} |x_k|^2 + \pi\Delta \left| \sum_{k=1}^{M} x_k \right|^2. \tag{17}$$

In terms of the original data x_k the formula (15), and, therefore, Eq. (13), will remain to be valid for computing $\langle G, B\rangle$, for the inner product automatically eliminates the role of s^-. That is, owing to the orthogonality property between the inner and outer Hardy spaces,

$$\langle s, B_n\rangle = \langle s^+, B_n\rangle + \langle s^-, B_n\rangle = \langle s^+, B_n\rangle = \langle G, B_n\rangle. \tag{18}$$

Once we have the decomposition for s^+, we have that for s by virtue of Equation (1).

An alternative algorithm strategy is to reduce the inner product (15) between the given analytic function G, or the Hardy space projection $G = s^+$ of the given nonanalytic signal s, and the entries B_k to one between some recursively induced analytic signals g_k and the evaluator $e_{\{a_k\}}$. The two strategies have their respective merits of which we refer to the fundamental literature [Qian, 2010] and [Qian and Wang, 2010].

3. The AFD Algorithm

Based on the described process, the flowchart of the AFD algorithm for analytic signals is shown in Fig. 1.

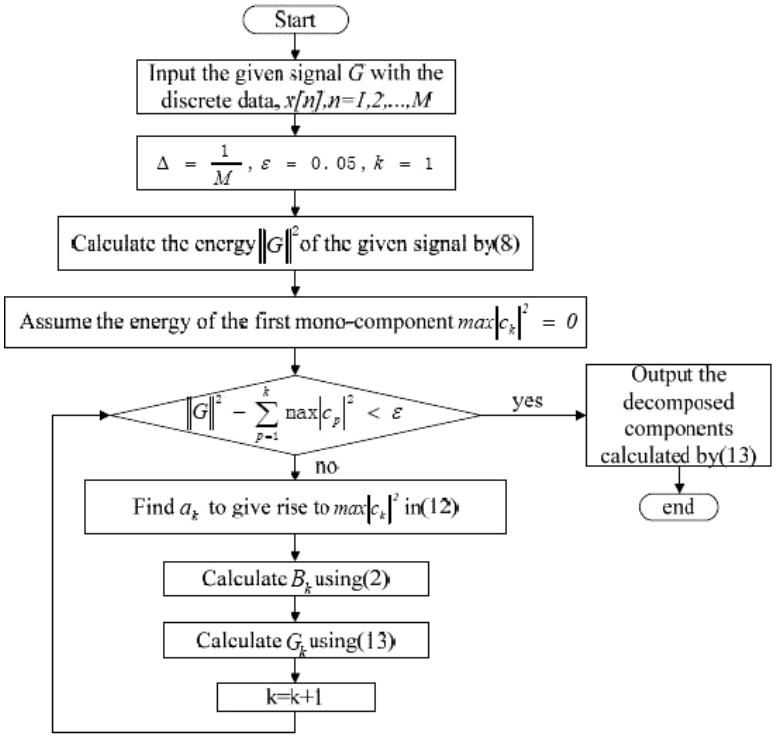

Fig. 1. Flowchart of AFD algorithm.

4. Experiment Results and Analysis

In this section, the effectiveness of the AFD is demonstrated by three signals. Here, the relative energy error of the Nth AFD partial sum is defined as

$$E_1(G;N) = \frac{\| G - G_N \|^2}{\| G \|^2}, \tag{19}$$

where $G_N = \sum_{p=1}^{N} C_p B_p$. In the same way, we have

$$E_2(F;N) = \frac{\| F - F_N \|^2}{\| F \|^2}, \tag{20}$$

where $F_N = \sum_{k=0}^{N} \langle F, f_k \rangle f_k$, and $f_k(e^{it}) = e^{ikt}$.

4.1. *Experiment* 1

The original signal (adapted from control theory) is

$$f_1 = \frac{0.0247z^4 + 0.0355z^3}{(1 - 0.9048z)(1 - 0.03679z)} \in H_2. \tag{21}$$

Figure 2 illustrates the real part of the original signal and those of the first to the sixth pre-mono-components through AFD. Figure 3 shows the partial sums of the corresponding pre-mono-components. Figure 4 shows the first to the fifth and the 26th partial sums through FD. Table 1 and Fig. 5 illustrate the comparison of

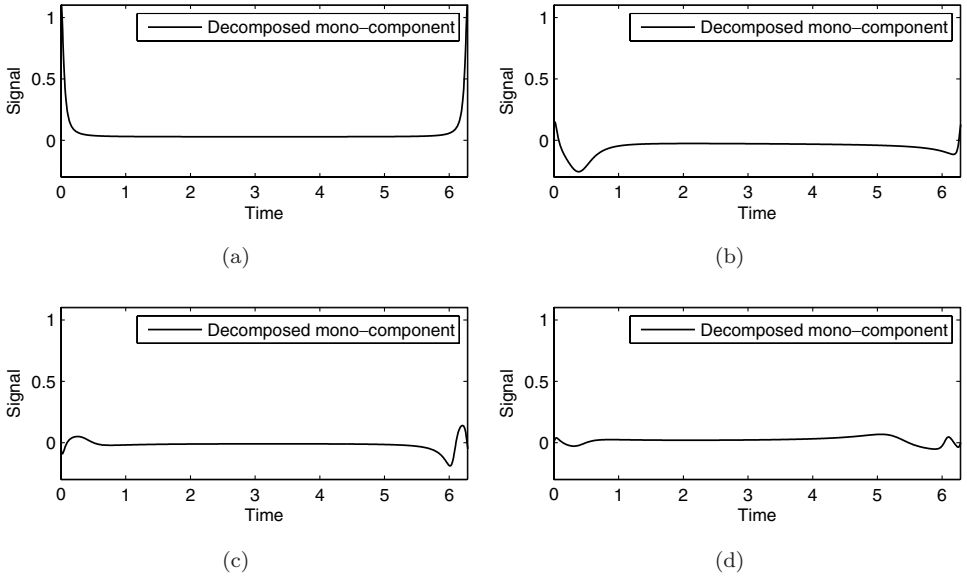

Fig. 2. The decomposing pre-mono-components of f_1: (a) the first pre-mono-component, (b) the second pre-mono-component, (c) the third pre-mono-component, (d) the fourth pre-mono-component, (e) the fifth pre-mono-component, and (f) the sixth pre-mono-component.

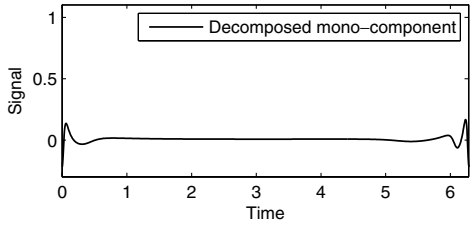

(e)

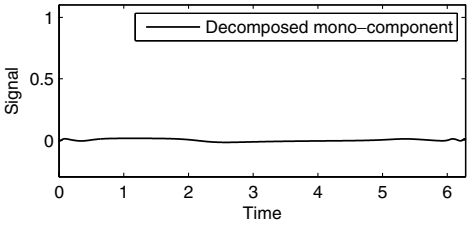

(f)

Fig. 2. (*Continued*)

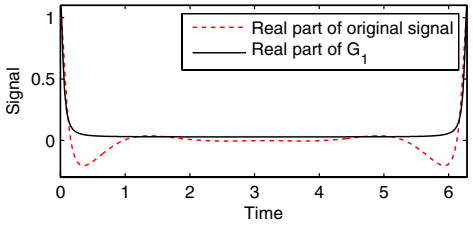

(a)

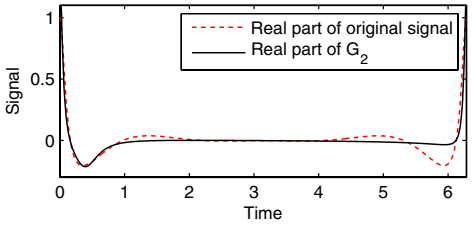

(b)

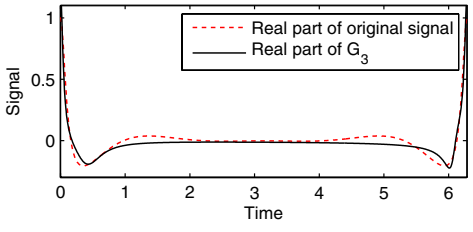

(c)

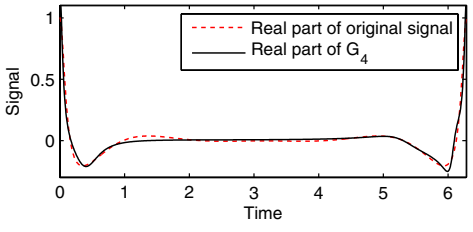

(d)

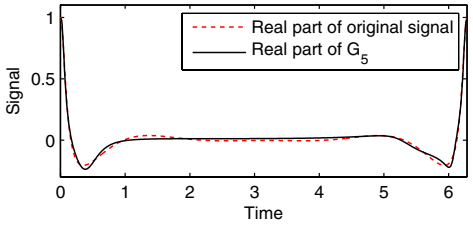

(e)

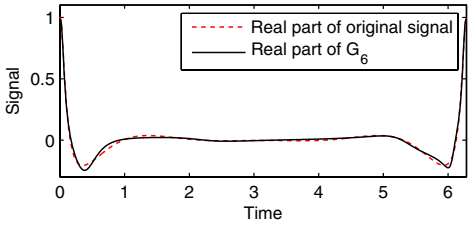

(f)

Fig. 3. AFDs of f_1: (a) the first AFD partial sum, (b) the second AFD partial sum, (c) the third AFD partial sum, (d) the fourth AFD partial sum, (e) the fifth AFD partial sum, and (f) the sixth AFD partial sum.

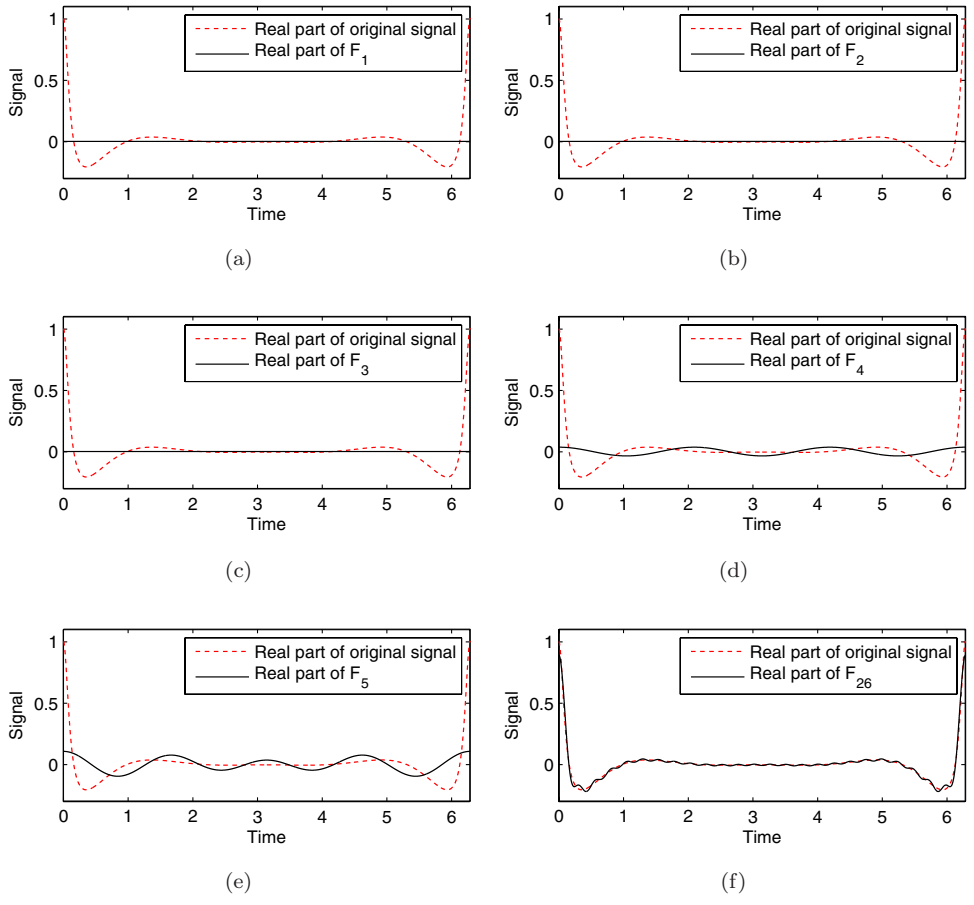

Fig. 4. Fourier decomposition of f_1: (a) the first FD partial sum, (b) the second FD partial sum, (c) the third FD partial sum, (d) the fourth FD partial sum, (e) the fifth FD partial sum, and (f) the 26th FD partial sum.

Table 1. Relative energy errors of f_1.

Method	First partial sum	Second partial sum	Third partial sum	Fourth partial sum	Fifth partial sum
FD	1.000	1.000	1.000	0.9721	0.8640
AFD	0.3799	0.1374	0.0825	0.0430	0.0138

the corresponding relative energy errors between AFD and FD. The results indicate that in term of relative energy error, it needs five-step decomposition in AFD to approximate the original signal, while it needs about 26-step decomposition in FD to achieve a compatible accuracy.

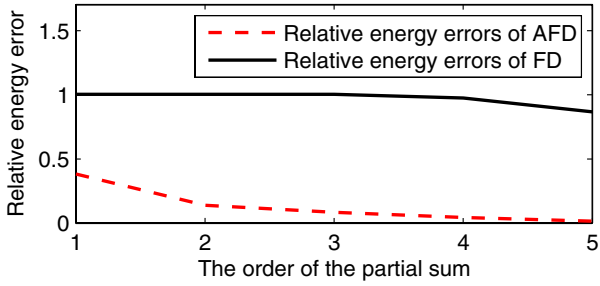

Fig. 5. Relative energy error curves of f_1.

4.2. *Experiment* 2

The original signal is

$$f_2 = \frac{1}{z^2 + 2} \in H_2. \tag{22}$$

Figure 6 illustrates the first four AFD partial sum approximations to f_2, and Fig. 7 shows the first to the third and the eighth Fourier partial sum approximations. The results indicate that in terms of relative energy error, it needs about three-step decomposition in AFD to approximate the original signal, while it needs

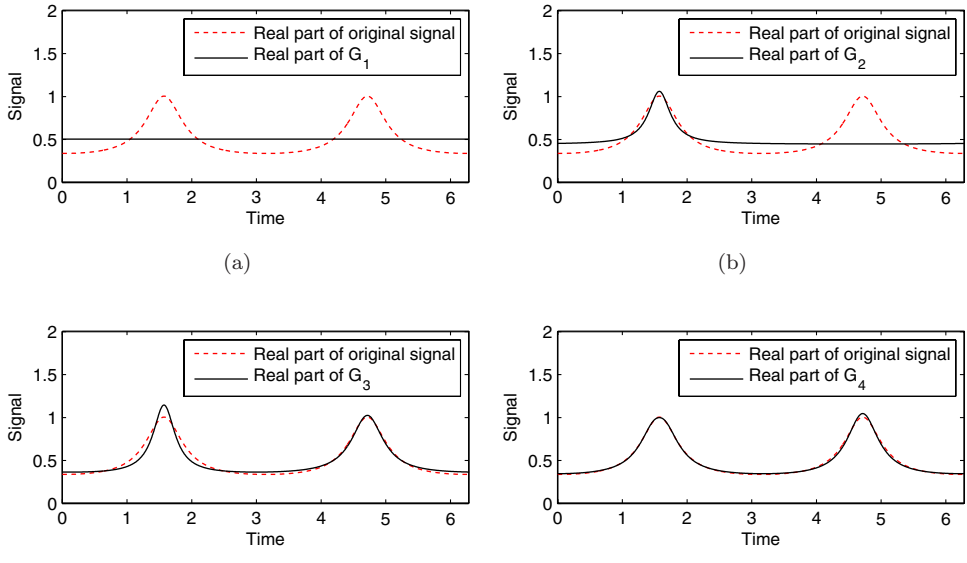

Fig. 6. AFD of f_2: (a) the first AFD partial sum, (b) the second AFD partial sum, (c) the third AFD partial sum, and (d) the fourth AFD partial sum.

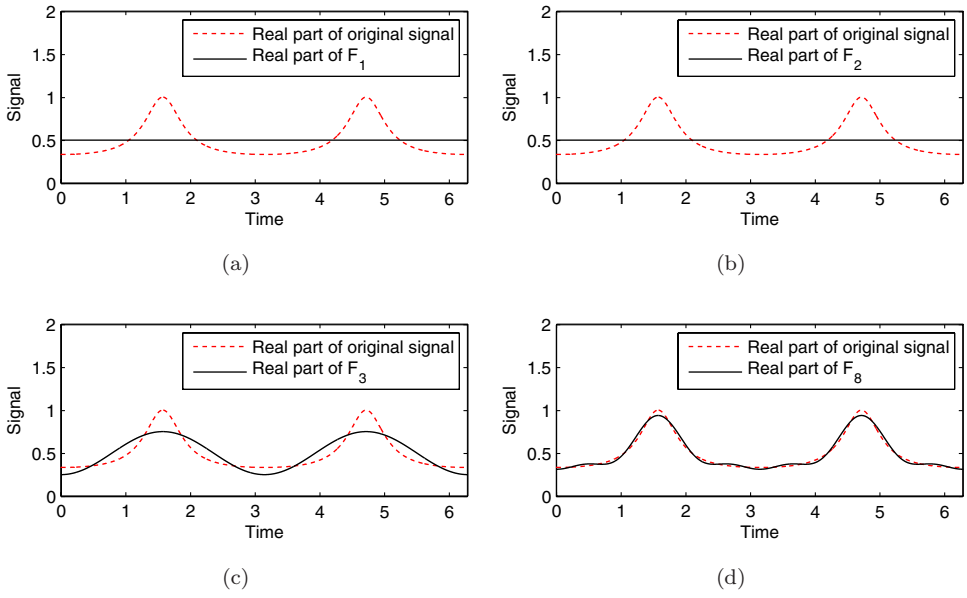

Fig. 7. Fourier decomposition of f_2: (a) the first FD partial sum, (b) the second FD partial sum, (c) the third FD partial sum, and (d) the eighth FD partial sum.

Table 2. Relative energy errors of f_2.

Method	First partial sum	Second partial sum	Third partial sum	Fourth partial sum	Fifth partial sum
FD	0.1429	0.1429	0.0357	0.0357	0.0089
AFD	0.1429	0.0893	0.0057	0.0005	0.0000

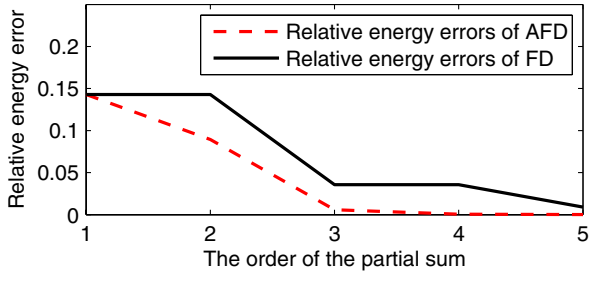

Fig. 8. Relative energy error curves of f_2.

about eight-step decomposition in FD to achieve a similar accuracy. Though in term of relative energy error FD also converges fast in this example, the pointwise approximation looks much more promising in the AFD approach. Table 2 and Fig. 8 show the comparison of relative energy errors between AFD and FD.

4.3. *Experiment* 3

The original signal is the chirp signal

$$f_3 = \cos t^2, \tag{23}$$

where $t \in [0, 2\pi]$. f_3 is a real-valued function. This signal can be processed according to Eq. (1).

Figure 9 is for the first, fourth, sixth, and eighth AFD partial sums, and Fig. 10 is for that of FD. The AFD algorithm seems to perform well in this example. Table 3 and Fig. 11 show the comparisons of the relative energy errors between AFD and FD. This experiment shows that the AFD algorithm can provide a much better approximation to the initial signal with less coefficients.

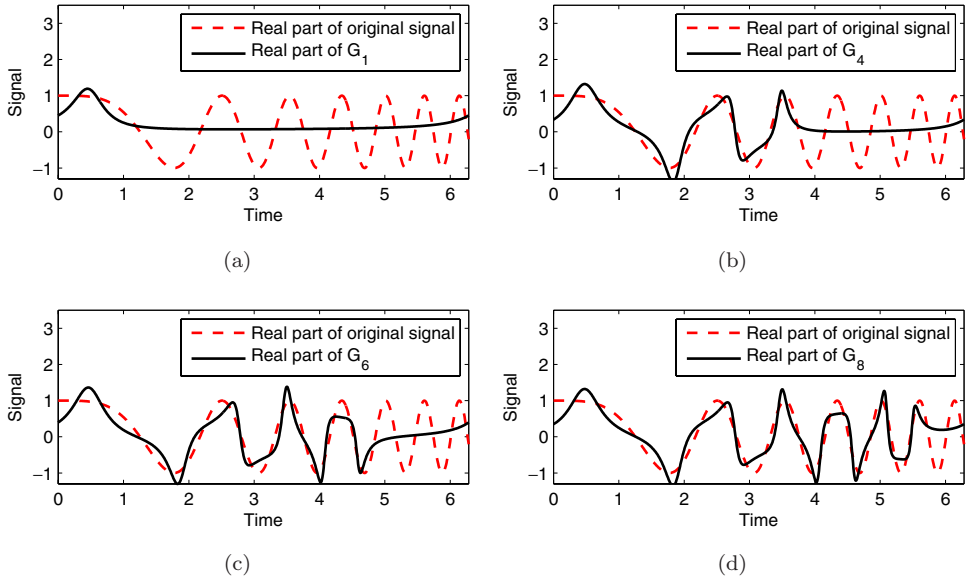

Fig. 9. AFD of f_3: (a) the first AFD partial sum, (b) the fourth AFD partial sum, (c) the sixth AFD partial sum, and (d) the eighth AFD partial sum.

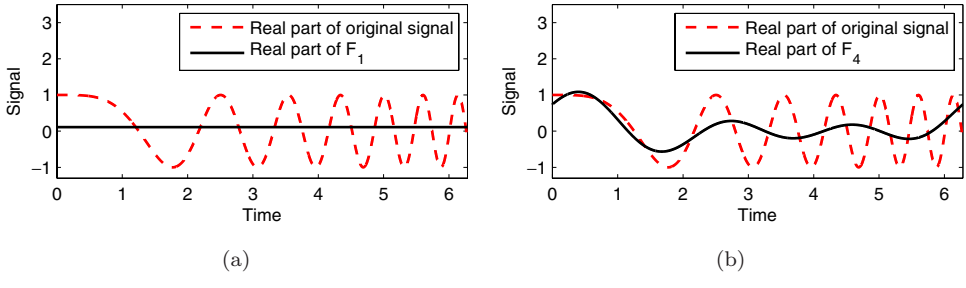

Fig. 10. Fourier decomposition of f_3: (a) the first FD partial sum, (b) the fourth FD partial sum, (c) the sixth FD partial sum, and (d) the eighth FD partial sum.

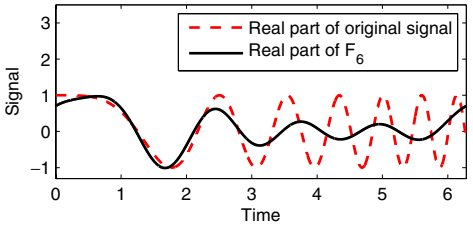

(c)

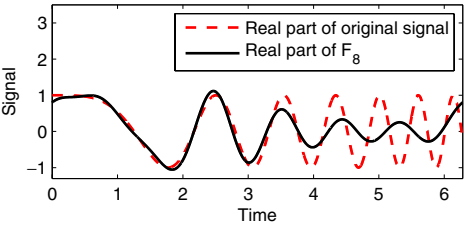

(d)

Fig. 10. (*Continued*)

Table 3. Relative energy errors of f_3.

Method	First partial sum	Fourth partial sum	Sixth partial sum	Eighth partial sum	Tenth partial sum
FD	0.9764	0.6545	0.5254	0.3627	0.1857
AFD	0.7965	0.4586	0.3217	0.2127	0.1135

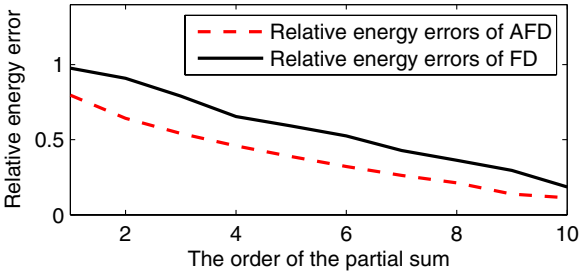

Fig. 11. Relative energy error curves of f_3.

5. Conclusion

AFD using rational orthogonal system is proposed. It is classified into the Fourier type because the basic signals are pre-mono-components or mono-components, those generalize the trigonometric functions Z^n. In the signal analysis, language mono-components are physically realizable signals with well-defined instantaneous frequencies. Signals with such properties are sought in time-frequency analysis. The adaptivity is in particular referred to fast convergence in energy. Here, the actual meaning of fast convergence is that a sum of a small number of pre-mono-components or mono-components will approximate the given signal to a promising accuracy.

The examples present that the proposed algorithm is efficiently effective. The algorithm is seen to be particularly suitable for signals consisting of low Fourier frequencies.

The computational complexity of the algorithm is to be further studied. The computation to find the maximal value of the particular differentiable function costs considerable time, and is to be simplified.

References

Akcay, H. and Niness, B. (1999). Orthonormal basis functions for modeling continuous-time systems. *Signal Process.* **77**: 261–274.

Bultheel, A. and Carrette, P. (2003). Takenaka-Malmquist basis and general Toeplitz matrices. *Proceedings of the 42nd CDC Conference*, Maui, Hawaii, Vol. 1, pp. 486–491, IEEE. Paper TuAPI.4.

Bultheel, A., Gonzalez-Vera, P., Hendriksen, E. and Njastad, O. (1999). *Orthogonal Rational Functions*, Vol. 5 of Cambridge Monographs on Applied and Computational Mathematics, Cambridge University Press, Cambridge.

Butzer, P. and Nessel, R. (1971). Fourier *Analysis and Approximation*, Volume 1: One-dimensional Theory, Birkhauser, Basel and Academic Press, New York.

Garnett, J. B. (1987). *Bounded Analytic Functions*, Academic Press, New York.

Mallat, S. and Zhang, Z. (1993). Matching pursuits with time-frequency dictionaries. *IEEE Trans. Signal Process.* **41**: 3397–3415.

Mi, W. and Qian, T. (2010). Frequency domain identification with adaptive rational orthogonal system. *Proceedings of 2010 International Conference on System Science and Engineering*, Taiwan.

Oppenheim, A. V. and Schafer, R. W. (2010). *Discrete-Time Signal Processing* (Third edition), Prentice Hall, Upper Saddle River, NJ.

Qian, T. (2006). Mono-components for decomposition of signals. *Math. Meth. Appl. Sci.* **29**: 1187–1198.

Qian, T. (2010). Mono-component decomposition of functions: An advance of Fourier theory. *Math. Meth. Appl. Sci.* **33**: 880–891.

Qian, T. and Wang, Y. B. (2010). Adaptive Fourier series — a variation of greedy algorithm. *Adv. Comput. Math.*, DOI 10.1007/s10444-01009153-4.

Rudin, W. (1996). *Real and Complex Analysis*, McGraw-Hill, New York.